European Journal of Neuroscience, pp. 1–15, 2018 doi:10.1111/ejn.13865

Correlates of economic decisions in the dorsal and subgenual anterior cingulate cortices

Habiba Azab[1] and Benjamin Y. Hayden[1,2]
[1]Department of Brain and Cognitive Sciences and Center for Visual Sciences, University of Rochester, Rochester, NY, 14618, USA
[2]Department of Neuroscience and Center for Magnetic Resonance Research, University of Minnesota, Minneapolis, MN, USA

Keywords: decision-making, macaca mulatta, reward, rhesus macaques, value

Abstract

The anterior cingulate cortex can be divided into distinct ventral (subgenual, sgACC) and dorsal (dACC), portions. The role of dACC in value-based decision-making is hotly debated, while the role of sgACC is poorly understood. We recorded neuronal activity in both regions in rhesus macaques performing a token-gambling task. We find that both encode many of the same variables; including integrated offered values of gambles, primary as well as secondary reward outcomes, number of current tokens and anticipated rewards. Both regions exhibit memory traces for offer values and putative value comparison signals. Both regions use a consistent scheme to encode the value of the attended option. This result suggests that neurones do not appear to be specialized for specific offers (that is, neurones use an *attentional* as opposed to *labelled line* coding scheme). We also observed some differences between the two regions: (i) coding strengths in dACC were consistently greater than those in sgACC, (ii) neurones in sgACC responded especially to losses and in anticipation of primary rewards, while those in dACC showed more balanced responding and (iii) responses to the first offer were slightly faster in sgACC. These results indicate that sgACC and dACC have some functional overlap in economic choice, and are consistent with the idea, inspired by neuroanatomy, which sgACC may serve as input to dACC.

Introduction

The dorsal (dACC) and subgenual (sgACC) anterior cingulate cortices are part of the cingulum, a band of grey matter located on the medial wall of the cerebral cortex that surrounds the corpus callosum (Heilbronner & Hayden, 2016). While the role of the dACC in value-based decision-making and reward processing has been studied for a long time (Niki & Watanabe, 1979; Ito *et al.*, 2003; Amiez *et al.*, 2005; Shidara & Richmond, 2002; Seo & Lee, 2007; Ebitz & Hayden, 2016), the role of the sgACC in this process has been examined only much more recently (Monosov & Hikosaka, 2012; Rudebeck *et al.*, 2014; Strait *et al.*, 2016; see also Amemori & Graybiel, 2012; who recorded in the adjacent pregenual cingulum, pgACC). Moreover, the precise roles of both regions in choice remain unclear. For example, some scholars view the dACC as being positioned outside of the choice process, either as a monitor and/or controller or as a downstream region (Shenhav *et al.*, 2013; Cai & Padoa-Schioppa, 2012; Blanchard & Hayden, 2014, 2015). Others view the dACC as a crucial part of the choice process (Bush *et al.*, 2002; Walton *et al.*, 2006; Croxson *et al.*, 2009; Wunderlich *et al.*, 2009; Hillman & Bilkey, 2010; Hare *et al.*, 2011; Boorman *et al.*, 2013; Grueschow *et al.*, 2015; Klein-Flugge *et al.*, 2016; Hayden *et al.*, 2011; Azab & Hayden, 2017). As another example, some scholars view sgACC as having a fundamentally limbic role, one that is presumably only tangentially related to choice (Bush *et al.*, 2000; Rudebeck *et al.*, 2014). Others have explored the roles of the sgACC as an economic region (Monosov & Hikosaka, 2012; and, for pgACC, Amemori & Graybiel, 2012).

More generally, the roles of these two regions in cognition are often thought of separately. While the dACC is closely associated with cognitive and executive functions (Devinsky *et al.*, 1995; Bush *et al.*, 2000; Rushworth *et al.*, 2002; for reviews see Shenhav *et al.*, 2013 and Heilbronner & Hayden, 2016), the sgACC is more closely associated with limbic processes (Drevets *et al.*, 1997; Botteron *et al.*, 2002; Rolls *et al.*, 2003; Coryell *et al.*, 2005; George *et al.*, 2006; Johansen-Berg *et al.*, 2008). Nonetheless, the two regions are closely interconnected, have many overlapping functional roles (Vogt *et al.*, 1992; Derbyshire *et al.*, 1998) and are both associated with mental disorders including depression (Mayberg *et al.*, 1997; Cotter *et al.*, 2001) as well as addiction (Forman *et al.*, 2004; Goldstein *et al.*, 2007). These facts, as well as their shared classification as cingulate cortex, support the idea that they may have some functional continuity.

Correspondence: H. Azab, as above. E-mail: hazab@ur.rochester.edu

Received 8 September 2017, revised 3 February 2018, accepted 5 February 2018

Edited by Dr. Thomas Klausberger. Reviewed by Johannes Passecker, Medical University of Vienna, Austria Ann Graybiel, Massachusetts Institute of Technology, USA

All peer review process communications can be found with the online version of the article.

Although the pre-frontal cortex as a whole can be subdivided into multiple functionally distinct anatomical regions (Rushworth *et al.*, 2011), a great deal of work suggests that there are some important functions that cross-regional boundaries (Fuster, 2001; Miller & Cohen, 2001; O'Reilly *et al.*, 2012; Wilson *et al.*, 2010). Economic choice and reward processing may be two of these functions (Schultz, 2000; O'Doherty, 2004; Rushworth *et al.*, 2011; Haber & Behrens, 2014). Given the evidence cited above, we believe the dACC and sgACC may jointly participate in economic processes. The aim of this study was to better characterize the neuronal responses associated with economic choice in these regions within the same task. Some of these results in dACC have been reported previously in Azab & Hayden, 2017. We reproduce them here for ease of comparison with sgACC findings, and note these explicitly in the results section.

Materials and methods

The task used here (Fig. 1A) was used in previous studies; some of the data analysed here were published (both regions in Strait *et al.*, 2016; only dACC data in Azab & Hayden, 2017). Analyses presented are novel, unless otherwise indicated in the results section.

Surgical procedures

All procedures were approved by the University Committee on Animal Resources at the University of Rochester and were designed and conducted in compliance with the Public Health Service's Guide for the Care and Use of Animals. Two male rhesus macaques (*Macaca mulatta*: subject B age 5 year 7 month; subject J age 6 year. 7 month at the start of recording) served as subjects in both studies. We used standard procedures, as described previously (Strait *et al.*, 2014). A small prosthesis for holding the head was used. Animals were habituated to laboratory conditions and then trained to perform oculomotor tasks for liquid reward. A Cilux recording chamber (Crist Instruments, Hagerstown, Maryland, USA) was placed over the dACC and attached to the calvarium with ceramic screws. Appropriate anaesthesia was used at all times; induction was performed with ketamine and isoflurane was used for maintenance. For surgical induction, we used 10–15 mg/kg of ketamine, 0.25 mg/kg of midazolam, and 2–4 mg/kg of propofol. For maintenance, we used isoflurane, ad lib level, set depending on active monitoring procedure. Animals received appropriate analgesics and antibiotics after all procedures. For systemic antibiotics, we used cefazolin and for topical application, we used standard veterinary triple antibiotic. For analgesics, we used meloxicam, and, when judged necessary by veterinary staff, buprenorphine. Post-operative care included close monitoring and restoration of fluid intake. Position of brain regions was verified by magnetic resonance imaging with the aid of a Brainsight system (Rogue Research Inc., Montreal, Quebec, Canada). Throughout both behavioural and physiological recording sessions, the chamber was kept sterile with regular antibiotic washes and sealed with sterile caps.

Recording site

We approached dACC through a standard recording grid (Crist Instruments). We defined dACC according to the Paxinos atlas (Paxinos *et al.*, 2000). Roughly, we recorded from a ROI lying within the coronal planes situated between 29.50 and 34.50 mm rostral to interaural plane, the horizontal planes situated between 4.12 and 7.52 mm from the brain's dorsal surface and the sagittal planes between 0 and 5.24 mm from medial wall (Fig. 1B). Our dACC recordings were made from a central region within this zone. We confirmed recording location before each recording session using our Brainsight system with structural magnetic resonance images taken before the experiment. Neuroimaging was performed at the Rochester Center for Brain Imaging, on a Siemens 3T MAGNETOM Trio Tim using 0.5 mm voxels. We confirmed recording locations by listening for characteristic sounds of white and grey matter during recording, which in all cases matched the loci indicated by the Brainsight system.

We approached sgACC using similar equipment, in a similar manner. We defined sgACC as lying within the coronal planes

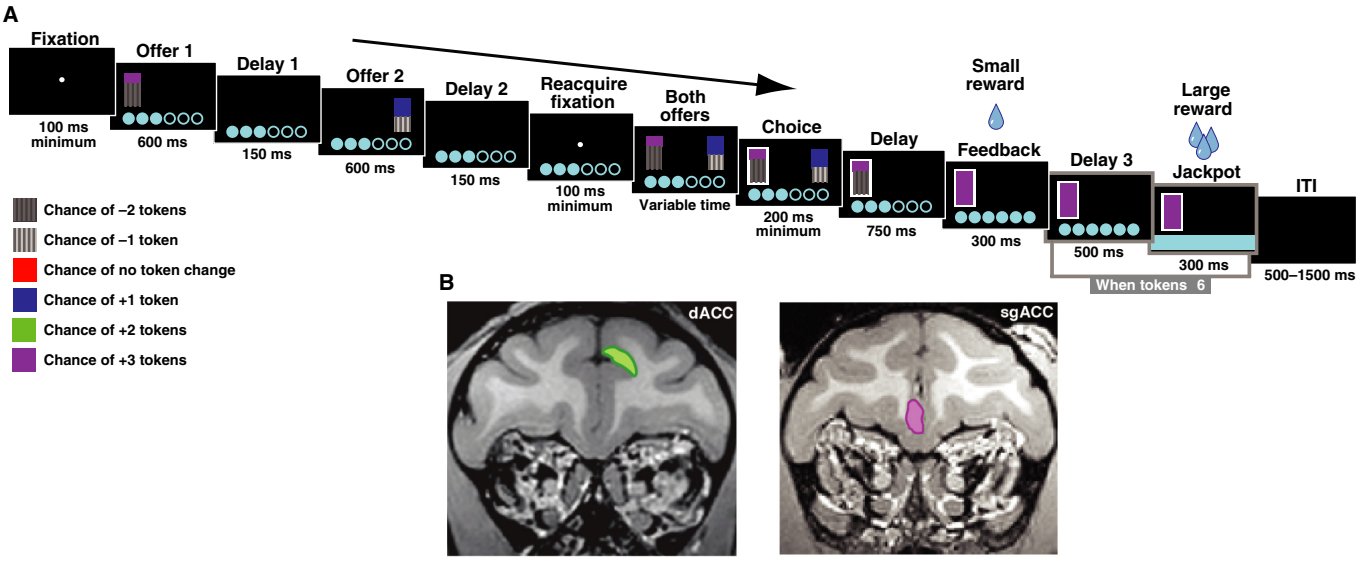

FIG. 1. (A) Example trial from token-gambling task. Offers were presented asynchronously, and the side the first offer appeared on was counterbalanced across trials. Each gamble offered one of two outcomes (indicated by the colours of the bars) at a certain probability (indicated by their heights). (B) Regions of interest (for exact coordinates, see Methods). Figure is reproduced from Azab & Hayden (2017), with an added panel for sgACC.

situated between 24 and 36 mm rostral to interaural plane, the horizontal planes situated between 17.33 and 25.12 mm from the brain's dorsal surface and the sagittal planes between 0 and 5.38 mm from the medial wall (Fig. 1B). Our sgACC recordings were made from a central region within this zone. We again confirm recording locations using structural magnetic resonance images, Brainsight, and listening to characteristic sounds of white and grey matter. These regions correspond to area 25 as identified by Paxinos (n = 118 cells) and also to the most caudal portion of area 32 (n = 28 cells).

Electrophysiological techniques

Single electrodes (Frederick Haer & Co., Bowdoin, Maine, USA; impedance range 0.8–4 MU) were lowered using a microdrive (NAN Instruments, Nazaret Illit, Israel) until waveforms of at least one neurone were isolated. Individual action potentials were isolated on a Plexon system (Plexon, Inc., Dallas, Texas, USA). Neurones were selected for study solely on the basis of the quality of isolation; we never pre-selected based on task-related response properties. All collected neurones for which we managed to obtain at least 250 trials were analysed. We collected 55/77 dACC/sgACC cells in subject B and 74/69 cells in subject J.

Eye tracking and reward delivery

Eye position was sampled at 1000 Hz by an infrared eye-monitoring camera system (SR Research, Ottawa, Ontario, Canada). Stimuli were controlled by a computer running Matlab (Mathworks, Natick, Massachusetts, USA) with Psychtoolbox (Brainard, 1997) and Eyelink Toolbox (Cornelissen *et al.*, 2002). Visual stimuli were coloured rectangles on a computer monitor placed 57 cm from the animal and centered on its eyes. A standard solenoid valve controlled the duration of juice delivery. The relationship between solenoid open time and juice volume was established and confirmed before, during and after recording.

Behavioural task

Monkeys performed a two-option gambling task (previously analysed for a narrower purpose in Strait *et al.*, 2016; and in Azab & Hayden, 2017 for dACC only). The task was similar to ones we have used previously (Blanchard *et al.*, 2014; Strait *et al.*, 2014, 2015; Blanchard & Hayden, 2015), with two major differences: (i) monkeys gambled for virtual tokens—rather than liquid—rewards, and thus (ii) outcomes could be losses as well as wins.

Two offers were presented on each trial. Each offer was represented by a rectangle 300 pixels tall and 80 pixels wide (11.35° of visual angle tall and 4.08° of visual angle wide). Twenty percentage of options were safe (100% probability of either 0 or 1 token), while the remaining 80% were gambles. Safe offers were entirely red (0 tokens) or blue (1 token). The size of each portion indicated the probability of the respective reward. Each gamble rectangle was divided horizontally into a top and bottom portion, each coloured according to the token reward offered. Gamble offers were thus defined by three parameters: two possible token outcomes and probability of the top outcome (the probability of the bottom was strictly determined by the probability of the top). The top outcome was 10%, 30%, 50%, 70% or 90% likely on gamble offers.

Six initially unfilled circles arranged horizontally at the bottom of the screen indicated the number of tokens to be collected before the subject obtained a liquid reward. These circles were filled appropriately at the end of each trial, according to the outcome of that trial. When six or more tokens were collected, the tokens were covered with a solid rectangle while a liquid reward was delivered. Tokens beyond six did not carry over, nor could number of tokens fall below zero.

On each trial, one offer appeared on the left side of the screen and the other appeared on the right. Offers were separated from the fixation point by 550 pixels (27.53° of visual angle). The side of the first offer (left and right) was randomized by trial. Each offer appeared for 600 ms and was followed by a 150 ms blank period. Monkeys were free to fixate upon the offers when they appeared (and in our observations almost always did so). After the offers were presented separately, a central fixation spot appeared and the monkey fixated on it for 100 ms. Following this, both offers appeared simultaneously and the animal indicated its choice by shifting gaze to its preferred offer and maintaining fixation on it for 200 ms. Failure to maintain gaze for 200 ms did not lead to the end of the trial, but instead returned the monkey to a choice state; thus, monkeys were free to change their mind if they did so within 200 ms (although in our observations, they seldom did so). A successful 200 ms fixation was followed by a 750 ms delay, after which the gamble was resolved and a small reward (100 μL) was delivered—regardless of the outcome of the gamble—to sustain motivation. This small reward was delivered within a 300 ms window. If six tokens were collected, a further delay of 500 ms was followed by a large liquid reward (300 μL) within a 300 ms window, followed by a random intertrial interval (ITI) between 0.5 and 1.5 s. If six tokens were not collected, subjects proceeded immediately to the ITI.

Each gamble included at least one positive or zero-outcome, ensuring that every gamble carried the possibility of a win (or at least no change in tokens). This decreased the number of trivial choices presented to subjects, and maintained motivation.

Statistical methods

Peri-stimulus time histograms (PSTHs) were constructed by aligning spike rasters to events of interest within the trial (namely, the presentation of the first offer or the presentation of feedback) and averaging firing rates across multiple trials. Firing rates were calculated in 20 ms bins but were generally analysed in longer epochs. For latency analyses, we used PSTHs with firing rates calculated in 5 ms bins to grant us finer resolution to detect shorter latencies.

Firing rates were normalized by subtracting the mean and dividing by the standard deviation of the neurone's entire PSTH (i.e. z-scoring).

Standard errors of the mean for all figures were computed over the average firing rate in the epoch of analysis over all trials within a task condition. These values are reported in the figure captions.

We tested for significant tuning and assessed variance explained using a multiple generalized linear regression model, including the following task-relevant variables: expected value (EV) of offers 1 and 2, the number of tokens collected as of the beginning of the trial, the side the first offer appeared on, the side of the chosen offer, the outcome of the trial (in tokens), the probability of that outcome (a measure of surprise) and whether this trial was a jackpot trial (where a large primary reward was delivered).

Analysis epochs were chosen a priori, before data analysis began, to reduce the likelihood of p-hacking, and so results were comparable to those previously published from our lab using similar tasks. The first and second offer epochs were defined as the 500 ms epoch beginning 100 ms after the offer was presented. The reward epoch was defined as the 700 ms epoch starting 100 ms following the

resolution of a gamble: this was when feedback and a small liquid reward were given (regardless of trial outcome), followed by a 500 ms delay (this was part or all of the ITI on non-jackpot trials, and a pre-jackpot delay on jackpot trials). These epochs were chosen before data collection began; indeed, they originally were selected for a previous study on a different brain region, and to account for hypothesized delays in neural responding (Strait *et al.*, 2014).

All fractions of neurones were tested for significance using a two-sided binomial test. All binomial tests throughout the article were two-sided. When testing for significant encoding in the population, we use an alpha level of 0.05 to indicate chance (i.e. the number of neurones that would exhibit significant modulation at random). When testing for (positive or negative) biases in the significantly modulated population, we use an alpha level of 0.5 to indicate chance (i.e. a perfectly balanced population).

We also tested for modulation biases across the entire population of neurones, rather than focusing simply on the significantly modulated population (i.e. neurones that cross the $P = 0.05$ threshold of significance). To do this, we use a Wilcoxon signed-rank test comparing a distribution of regression coefficients to zero; the non-parametric counterpart to a one-sample *t*-test. The corresponding *Z*-statistic can be interpreted similar to the *T*-statistic: with positive values indicating positively skewed distributions, and negative values indicating negatively skewed distributions.

Format and population correlation analyses were performed in the following manner. We use beta correlation analyses to assess whether neurones represented two variables (or the same variable at different time periods) using similar/orthogonal/opposing formats, in overlapping/orthogonal/distinct populations. To do this, we first found the regression coefficient associated with the variable of interest per neurone. We estimate this using a multiple linear regression model, as described above. We then combined the regression coefficients associated with the variable of interest into a vector of the same length as the number of neurones in our sample. This vector indicates the relative strength (after normalizing) and direction of modulation for each individual neurone in the population, in response to a particular variable in a particular epoch. We call this the population 'format'. We compared different formats by finding the Pearson's correlation coefficient between them. This method has been used in previous studies, both from our own laboratory (Strait *et al.*, 2014, 2015; Blanchard *et al.*, 2015) as well as others (Kriegeskorte *et al.*, 2008; Mante *et al.*, 2013; Stokes *et al.*, 2013; Donahue & Lee, 2015).

Note that this approach provides a more sensitive method of examining population properties than conventional approaches, which involve determining which cells cross a significance threshold and then using those as focal cells for further analyses. By taking on all cells regardless of their response, our method accomplishes two purposes. First, it uses all available information, even information that is not sufficient by itself to achieve significance. Second, it avoids introducing a hard categorical boundary, which can introduce false positives in data (Maxwell & Delaney, 1993; Blanchard *et al.,* 2018).

We extend this method to account for the noise inherent in estimating each neurone's encoding of each variable of interest, which existing methods do not account for (Azab & Hayden, 2017). We used a Bayesian regression to obtain a probabilistic distribution over each regression coefficient for each neurone (rather than an individual coefficient estimate per neurone; this is akin to taking into account the confidence interval on each regression coefficient estimate). We sampled 10 000 regression coefficients from this distribution for each neurone, to obtain a probability distribution of (10 000) potential formats for the population, for each of two task conditions. We then performed the correlation analyses on each of these samples across task conditions, thus generating a probability distribution of (10 000) correlation coefficients. This is a more robust estimate of the correlation between formats, as it takes into account the uncertainty inherent in estimating any individual regression coefficient, and allows us to view the spread of the distribution of this correlation when this significant source of noise is taken into account. 99% credible intervals allowed us to estimate the likely range of the correlation coefficients with 99% certainty.

The Pearson's correlation coefficient between signed regression coefficients indicated whether variables were represented in a similar format, that is directionality of tuning across the population. A positive correlation indicated a preservation of directionality, while a negative correlation suggested variables were represented in opposing directionality of firing rate modulation. No correlation suggests orthogonal formats, but we draw no strong conclusions from these.

Similarly, the Pearson's correlation coefficient between unsigned regression coefficients indicated whether similar neuronal populations tended to be involved in encoding the two variables in question, regardless of their direction of modulation. A positive correlation indicated overlapping populations, while a negative correlation indicated separate ones. A lack of correlation suggests orthogonal populations (i.e. encoding one variable does not affect the neurone's likelihood of encoding the other variable); however, we again draw no strong conclusions from this result.

To perform our latency analysis, we used a multiple linear regression model (described above) to predict firing rates in a 500 ms sliding window throughout the course of the trial. We obtained the fraction of variance explained (i.e. R^2) by this full model at each point of time for each neurone in sgACC and dACC. We then removed one of these variables to estimate the fraction of variance it uniquely explained in each brain region at each point of time. To avoid the potential confounding factor of less signal in sgACC, we looked at the time of peak variance explained in each brain region for each neurone for each of the variables, and compared these time points using a (non-parametric) Wilcoxon rank-sum test. This method allows us to determine whether the peak activity in response to a particular variable occurs earlier in one region compared to the other across the entire population. We performed this analysis for each variable on all neurones in the population, and again on only those neurones that were significantly modulated by a particular variable.

Results

Task structure and behaviour

Two male rhesus macaques performed a token-gambling task. On each trial, subjects chose between two options presented asynchronously that differed in three dimensions: win amount, loss amount and probability of win (Fig. 1A). Both subjects showed behaviour consistent with task understanding (Fig. 2). Specifically, both subjects preferred the option with the greater mathematical expected value significantly more often than chance (subject B: 80.3%; subject J: 75.1%; two-sided binomial test: both $P < 0.0001$) and were sensitive to all three parameters that defined each gamble (see Table 1). Subjects were more sensitive to win amount than to loss amount (where 'losses' are defined as the smaller outcome of a gamble even if it led to a gain of tokens; two-sample *t*-test comparing unsigned regression coefficients for wins and losses for each gamble: left gamble: $P = 4.05 \times 10^{-31}$ and $P = 3.38 \times 10^{-38}$, right gamble: $P = 1.13 \times 10^{-32}$ and $P = 1.64 \times 10^{-41}$ for subjects

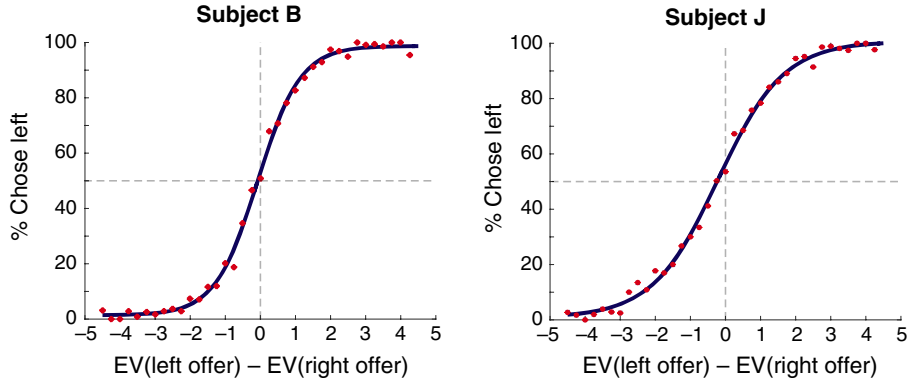

FIG. 2. Behaviour for each subject, fit to a sigmoid function. Subjects choose the left option more often as its value increases, as would be expected given understanding of the task. EV: expected value of gamble. Figure is reproduced from Azab & Hayden (2017).

TABLE 1. Subjects' choices were influenced by all values characterizing both gambles. Average regression coefficients from a multiple logistic regression model of choice (left = 1, right = 0) against the variables in the regressor column, for each behavioural session. The distribution of regression coefficients across sessions for every behavioural variable listed deviated significantly from zero. A 'loss' within a gamble was always less than or equal to the win outcome of that gamble, and may or may not be a negative value. The magnitude of the regression coefficient indicated the extent to which this variable influenced choice, while its sign indicated whether higher values of this variable (positive vs. negative) favoured choice of the left vs. right gamble, respectively.

	Subject B (n = 66 sessions)		Subject J (n = 74 sessions)	
Regressor	Mean regression coefficient	Wilcoxon sign-rank Z-statistic (P-value)	Mean regression coefficient	Wilcoxon sign-rank Z-statistic (P-value)
Left offer –win	1.40	7.06 ($P = 1.64 \times 10^{-12}$)	1.15	7.47 ($P = 7.773 \times 10^{-14}$)
Left offer –loss	0.486	6.97 ($P = 3.26 \times 10^{-12}$)	0.293	7.22 ($P = 6.35 \times 10^{-13}$)
Left offer –probability of win	5.12	7.06 ($P = 1.64 \times 10^{-12}$)	3.70	7.47 ($P = 7.73 \times 10^{-14}$)
Right offer –win	−1.33	−7.06 ($P = 1.65 \times 10^{-12}$)	−1.33	−7.47 ($P = 1.67 \times 10^{-12}$)
Right offer –loss	−0.412	−6.83 ($P = 8.37 \times 10^{-12}$)	−0.237	−7.06 ($P = 1.67 \times 10^{-12}$)
Right offer –probability of win	−4.85	−7.06 ($P = 1.64 \times 10^{-12}$)	−4.09	−7.47 ($P = 7.73 \times 10^{-14}$)

B and J, respectively), consistent with the idea that their choices reflect a focus on the win (Hayden & Platt, 2007; Hayden *et al.*, 2008). Monkeys showed weak side and order biases (leftward choice: 49.0% and 52.6%; preference for first option: 47.6% and 44.5% in subjects B and J, respectively; two-sided binomial test: all $P < 0.0001$).

Monkeys were risk-seeking; this pattern is consistent with several earlier studies (Hayden *et al.*, 2008; Hayden & Platt, 2009; McCoy & Platt, 2005). To assess risk-seeking, we fit a utility curve distortion parameter to subjects' behaviour in each session (Yamada *et al.*, 2013; Lak *et al.*, 2014). This parameter, α, was greater than 1 in both subjects (subject B: average $\alpha = 1.61$, $n = 66$ sessions; subject J: average $\alpha = 1.81$, $n = 74$ sessions); and in individual sessions (one-sample t-test over sessions, subject B: $T = 30.0$, $P = 9.35 \times 10^{-40}$; subject J: $T = 27.0$, $P = 9.18 \times 10^{-40}$). Subjects' behaviour was modestly influenced by the number of current tokens: accuracy improved as tokens increased (logistic regression of accuracy against tokens acquired for each session: subject B ($n = 66$ sessions): average $\beta = 0.0293$, $P = 0.00405$; subject J ($n = 74$ sessions): average $\beta = 0.0805$, $P = 1.53 \times 10^{-14}$).

Neurones in both regions encode the value of the first offer while it is attended

We collected 55 dACC and 77 sgACC cells in subject B, and 74 dACC and 69 sgACC cells in subject J. Responses of two example neurones (one in dACC and one in sgACC) are shown in Fig. 3A and B, respectively. Both of these neurones' firing rates were correlated with the expected value of the first offer while it was displayed on the screen. The firing rate of the dACC neurone was also affected by the expected value of the first offer when the second offer appeared. This was not the case for the sgACC neurone.

Significant proportions of neurones in both regions encoded the value of the first offer in the 500 ms epoch starting 100 ms after that offer appeared (epoch 1). We found that responses of 24.0% ($n = 31/129$) of neurones in dACC and 11.0% ($n = 16/146$) in sgACC were affected by the value of offer 1 during epoch 1. Both proportions are greater than chance (two-sided binomial test, dACC: $P = 2.33 \times 10^{-13}$; sgACC: $P = 0.00275$). Similar analyses for dACC neurones were reported in a previous article (Azab & Hayden, 2017).

Figure 3C shows the proportion of neurones whose firing rates were modulated by offer 1 value through time. There was no measured bias towards a positive direction in either area (see Table 2). We next sought to measure this effect across the entire population of neurones, to avoid excluding ones that carry information simply due to their failure to reach statistically significant modulation. We do this by comparing the strength and direction of modulation (i.e. the signed regression coefficients) of all neurones in response to a variable of interest (here, offer 1 value) against a default distribution centered around zero (see Methods). We still find no detectable bias in modulation in either brain region using this more sensitive measure (see Table 3).

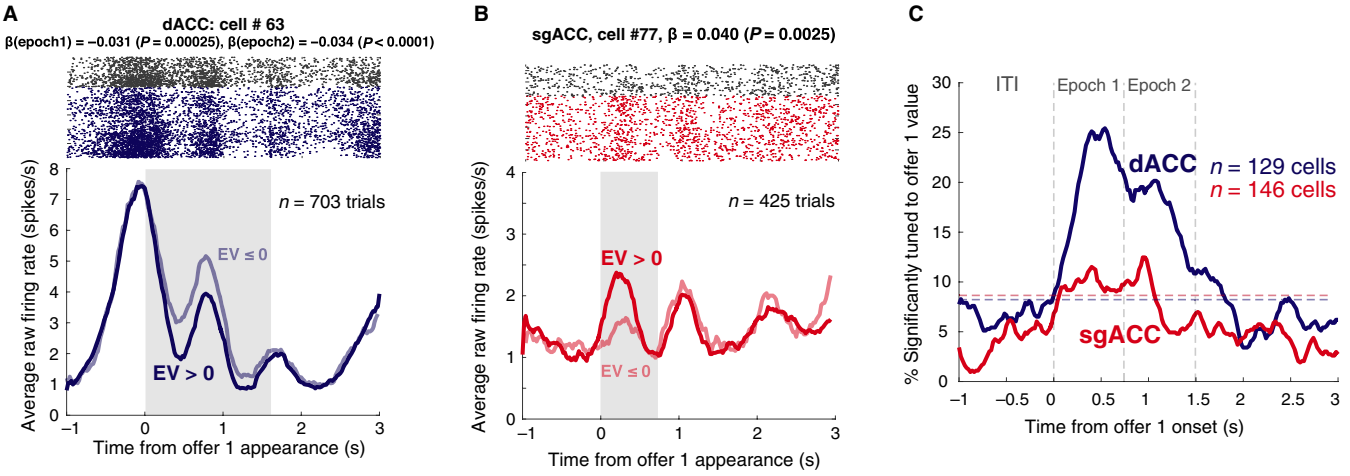

FIG. 3. Neural responses to the value of offer 1. All standard errors of the mean were computed for the epoch of analysis (see main text and Methods). (A) Responses of one dACC neuron with increasing firing rate in response to smaller values of offer 1 in both the first and second epochs. The first epoch begins 100 ms after the first offer appears, and lasts 500 ms; the second epoch begins 100 ms after the second offer appears, and lasts 500 ms. Grey region: total time where offers 1 and 2 were displayed on the screen (i.e. when offer 1 was attended and remembered). Standard error of the mean for positive-value trials = 0.122; standard error of the mean for negative-value trials = 0.192. (B) Responses of one sgACC neuron with increasing firing rates in response to larger values of offer 1 in the first epoch Grey region: total time where offer 1 was displayed on the screen. Standard error of the mean for positive-value trials = 0.128; standard error of the mean for negative-value trials = 0.187. (C) Proportion of neurons selective for the value of offer 1 in both regions throughout the course of the trial. This fraction was computed by regressing firing rate over a 500 ms sliding window against the expected value of the first offer, along with other task-relevant variables (see Methods), with data-points centered around this window. The blue and red dashed lines indicate the percentage of neurons we would expect to see by chance for dACC and sgACC, respectively (as determined by a two-sided binomial test, according to the number of cells in each area). A similar slidingwindow analysis for dACC is shown in Azab & Hayden (2017).

TABLE 2. Assessment of biases in frequency of coding in the significantly modulated population of neurones. We determine whether the fraction of positively tuned neurones (of the tuned population only) is significantly larger (or smaller) than chance (50%), using a two-sided binomial test. Significant proportions are shown in bold.

Variable	dACC (% positive)	sgACC (% positive)
Offer 1 value (attended)	51.6% (n = 16/31, P = 1.00)	68.8% (n = 11/16, P = 0.210)
Offer 1 value (remembered)	55.6% (n = 15/27, P = 0.701)	45.5% (n = 5/11, P = 1.00)
Offer 2 value (attended)	64.7% (n = 11/17, P = 0.332)	58.3% (n = 7/12, P = 0.774)
Outcome	**68.6% (n = 24/35, P = 0.0410)**	**18.1% (n = 4/22, P = 0.00434)**
Number of tokens	55.0% (n = 22/40, P = 0.636)	28.6% (n = 4/14, P = 0.180)
Jackpot	60.4% (n = 29/48, P = 0.193)	**83.3% (n = 15/18, P = 0.00754)**

TABLE 3. Assessment of biases in modulation in the overall neuronal population. We performed this analysis running a one-sample Wilcoxon signed-rank test on the regression coefficients corresponding to each variable obtained from a multiple linear regression (see Methods). Significant statistics are shown in bold. A positive/negative Z-statistic indicates a positively/negatively skewed distribution, respectively.

Variable	dACC Sign-rank test statistic Z-statistic (P-value)	sgACC Sign-rank test statistic Z-statistic (P-value)
Offer 1 value (attended)	−0.347 (P = 0.729)	1.474 (P = 0.141)
Offer 1 value (remembered)	−0.958 (P = 0.338)	−0.644 (P = 0.520)
Offer 2 value (attended)	0.403 (P = 0.687)	0.960 (P = 0.337)
Outcome	1.799 (P = 0.0720)	**−3.54 (P = 0.000408)**
Number of tokens	0.405 (P = 0.685)	**−2.42 (P = 0.0155)**
Jackpot	1.402 (P = 0.161)	**4.15 (P = 3.38 × 10^{-5})**

dACC neurones significantly encode the value of the second offer while it is attended

We next explored the effects of the second offer value on firing rates during epoch 2. Fig. 4A and B show two example neurones, one from dACC and one from sgACC, whose firing rates increased in response to the second offer. A significant proportion of neurones in dACC encoded the value of the second offer when it appeared (dACC: 14.0%, n = 18/129; two-sided binomial test: $P = 8.09 \times 10^{-5}$), although this proportion did not achieve significance in sgACC (8.22%, n = 12/146; two-sided binomial test: P = 0.0843). Similar results were reported for dACC neurones in a previous article (Azab & Hayden, 2017). There was no significant bias in tuning in either area: neither within the population of significantly tuned neurones (Table 2), nor across the entire population (using the more sensitive measure explained above; Table 3). Figure 4C shows how the fraction of neurones responsive to offer 2 changes over the course of the trial.

Memory traces of offer value

We next examined whether firing rates reflected the value of the first offer while the second offer was presented (epoch 2; 500 ms epoch starting 100 ms after the second offer appeared). We saw encoding of offer 1 in this epoch in dACC (20.9% of neurones, n = 27/129, two-sided binomial test: $P = 2.33 \times 10^{-10}$), but it failed to reach significance in sgACC (7.53%, n = 11/146, two-sided binomial test: P = 0.178). Similar results for the dACC population were reported in a previous article (Azab & Hayden, 2017). As task-relevant signals were generally attenuated in sgACC, we repeated this analysis in an earlier 500 ms epoch, starting immediately when the second

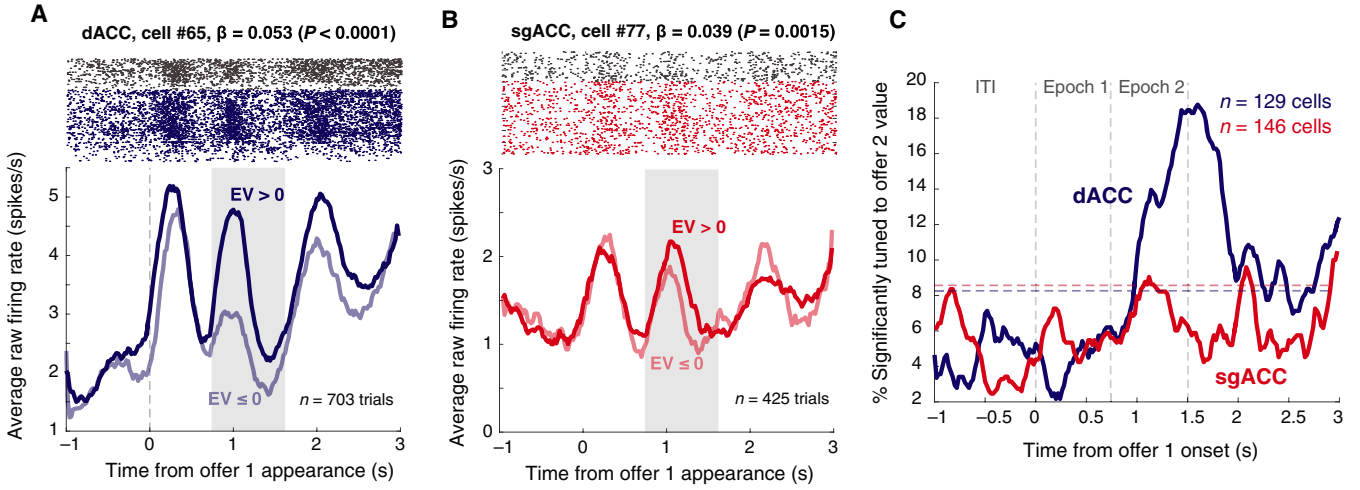

FIG. 4. Neural responses to the value of offer 2. Grey shaded regions indicate the time when offer 2 was displayed on the screen. All standard errors of the mean were computed for the epoch of analysis (see main text and Methods). (A) Responses of one dACC cell whose firing rate increased in response to larger values of offer 2. Standard error of the mean for positive-value trials = 0.180; standard error of the mean for negative-value trials = 0.225. (B) Responses of one sgACC cell whose firing rate increased in response to larger values of offer 2. Standard error of the mean for positive-value trials = 0.122; standard error of the mean for negative-value trials = 0.213. (C) Percentage of cells tuned to the value of the second offer in both regions over the course of the trial. A 500 ms sliding window was used to compute these values at each point of the trial, with data-points centered around this window. The blue and red dashed lines indicate the percentage of neurons we would expect to see tuned by chance (as determined by a two-sided binomial test, according to the number of cells in each area) for dACC and sgACC, respectively. A similar slidingwindow analysis was shown in Azab & Hayden (2017).

offer appeared. The fraction of neurones tuned to the value of offer 1 in this epoch does achieve significance (11.6%, n = 17/146, two-sided binomial test: P = 0.00107). This proportion is still significant after a Bonferroni correction for multiple comparisons (i.e. at $P < 0.025$). This finding suggests that sgACC may, in fact, carry a memory signal, although one that is more attenuated and less reliable than that in dACC. This result should be interpreted with caution: further studies are required to corroborate this finding.

Neurones in both regions integrate gamble probability and stakes

In our task, the value of an offer was determined by three factors: the probability of the win, the win amount, and the loss amount (the probability of the loss was entirely determined by the probability of the win). We investigated whether these variables were integrated into a unified value signal, or represented orthogonally.

Value is determined by a systematic combination of stakes and probability; if neurones encode value (and not just its components), their response functions for these individual variables will be related. We focused on the first epoch of the trial to reduce possible choice-related effects associated with the appearance of the second offer. We compared regression weights for neuronal responses to the win portion of the first offer (i.e. the ensemble *format* for wins) against the regression weights characterizing neuronal responses to the loss portion of the first offer, and the probability of a win in the first offer.

Previous studies have characterized this ensemble format as the vector of (signed) regression coefficients; one for each neurone in response to a particular variable of interest during a particular epoch (Kriegeskorte *et al.*, 2008; Mante *et al.*, 2013; Stokes *et al.*, 2013; Donahue & Lee, 2015). We extend this analysis to account for the noise in these individual regression coefficients. Rather than obtaining a single estimate for each regression coefficient for each neurone, we compute a likely *distribution* of this coefficient given the noise in each individual neurone's data. Therefore, across the population, we obtain a probability distribution of vectors or tuning formats that characterizes the population's response to a particular variable. We can then correlate the individual samples that make up this distribution between two different task conditions (these could be two different variables, or the same variable at two different time points). This method gives us an estimate of the likely correlation between tuning formats in a population, while taking into account the noise at the level of individual neurones: a source of noise previous methods do not account for (for more detail, see Methods).

Using this method, we find a distribution of positive correlations between the regression coefficients corresponding to win-magnitude and win probability, supporting the hypothesis that these parameters are integrated. This correlation is observed in both cingulate regions (dACC: average Pearson's correlation coefficient r = 0.279, 99% credible interval = [0.208, 0.350]; sgACC: r = 0.212, 99% credible interval = [0.126, 0.299]; note that neither of these intervals contains 0, suggesting a positive correlation with 99% confidence).

We also tested whether these variables were integrated by determining whether they were encoded by overlapping neuronal populations. We achieve this by finding the correlation between the unsigned regression coefficients, thus measuring the strength of modulation and ignoring its sign. A positive correlation of absolute values indicates that the neurones that strongly encode one variable are more likely to strongly encode the other, and vice versa. That is, the positive correlation of absolute values is a signature that the two variables are encoded by largely overlapping populations of cells. (This method is conceptually similar to, but more sensitive than, the approach of counting the number of cells significant for both variables, as in a Venn diagram. For further detail, see Methods). These results thus indicate that win probability and win amount were encoded by a single population of neurones rather than two distinct ones —further supporting the integration hypothesis (dACC:

$r = 0.321$, 99% credible interval = [0.222, 0.417]; sgACC: $r = 0.384$, 99% credible interval = [0.275, 0.487]). We previously reported similar findings in the ventromedial pre-frontal cortex (vmPFC) and the ventral striatum (VS, Strait *et al.*, 2015). These results suggest that these cingulate regions also carry integrated value signals.

Win and loss magnitudes were also integrated in both areas (dACC: $r = 0.332$, 99% credible interval = [0.258, 0.405]; sgACC: $r = 0.448$, 99% credible interval = [0.368, 0.524]). These values were represented in significantly overlapping populations in both cingulate regions (dACC: $r = 0.153$, 99% credible interval = [0.0403, 0.2606]; sgACC: $r = 0.212$, 99% credible interval = [0.0876, 0.339]). These findings further support the integration hypothesis.

Consistent ensemble tuning patterns for attended and remembered values in both cingulate regions

We next investigated the relationship between the tuning format for attended and for remembered offers. In particular, we wanted to know whether the value of offer 1 was encoded in similar tuning formats as it moved from the visual field to working memory. Our findings support this hypothesis for both regions. Findings for dACC using a similar analysis were reported in a previous article (Azab & Hayden, 2017).

Using the same method outlined above, we find a positive correlation between the format of offer 1 value when it is attended and when it is remembered, suggesting some continuity in the representation of this value in the neuronal population. This result holds in both brain regions (dACC: $r = 0.349$, 99% credible interval = [0.286, 0.411]; sgACC: $r = 0.190$, 99% credible interval = [0.100, 0.274]; Fig. 5). We then considered whether attended and remembered values used same neuronal population. To do so, we correlated unsigned regression coefficients. These values were positive in both cingulate regions, indicating overlapping populations (dACC: $r = 0.455$, 99% credible interval = [0.365, 0.543]; sgACC: $r = 0.280$, 99% credible interval = [0.162, 0.397]).

A putative signature of mutual inhibition between offer values in both cingulate regions

We apply the same method of analysis to address two more hypotheses. First, we wondered how the coding formats for the two offers after they have both been presented (and are, presumably, being compared) related to each other. One putative neural signature of the comparative process is mutual inhibition: an anti-correlation between regression coefficients for the values of the two offers while they are being compared (Strait *et al.*, 2014). This anti-correlation indicates that the two offers modulate neuronal activity in opposing directions, and that the ensemble of neurones effectively subtracts their values. We observe this pattern in both cingulate regions (dACC: $r = -0.151$, 99% credible interval = [−0.229, −0.0742]; sgACC: $r = -0.151$, 99% credible interval: [−0.239, −0.0580]; Fig. 6). Qualitatively similar results were observed in dACC using a similar analysis, reported in a previous article (Azab & Hayden, 2017). Note that, despite the higher level of noise in sgACC, our method allows us to retrieve the same strength of signal from both regions, albeit with a larger confidence interval for the sgACC measure. We also considered whether these comparison signals were carried by overlapping populations, and find this to be the case in both regions (dACC: $r = 0.203$, 99% credible interval = [0.0996, 0.308]; sgACC: $r = 0.194$, 99% credible interval = [0.0681, 0.314]). These findings suggest that both regions carry correlates of value comparison, despite weak offer value signals in sgACC during this time period.

Consistent ensemble tuning patterns for different attended values in both cingulate regions

Finally, we sought to determine whether cingulate regions encode all attended offers similarly, and using the same population. Our previous studies of vmPFC and VS indicate that value coding in these regions is attentionally aligned—that is, they encode the value of the attended offer in a consistent format. This framework differs from a labelled line format, in which a specialized set of neurones encodes the value of each offer, respectively (e.g. Hunt *et al.*, 2012; Rustichini & Padoa-Schioppa, 2015; for a detailed discussion, see Azab & Hayden, 2017). We compared the regression coefficients associated with the first offer in the first epoch to those associated with the second offer in the second epoch. Our data support the attentional alignment hypothesis. Specifically, coding direction for both offers was consistent in both areas (dACC: $r = 0.343$, 99% credible interval = [0.273, 0.409]; sgACC: $r = 0.207$, 99% credible interval = [0.119, 0.293]; Fig. 7). Both regions also made use of overlapping (i.e. correlated) sets of neurones to encode the two

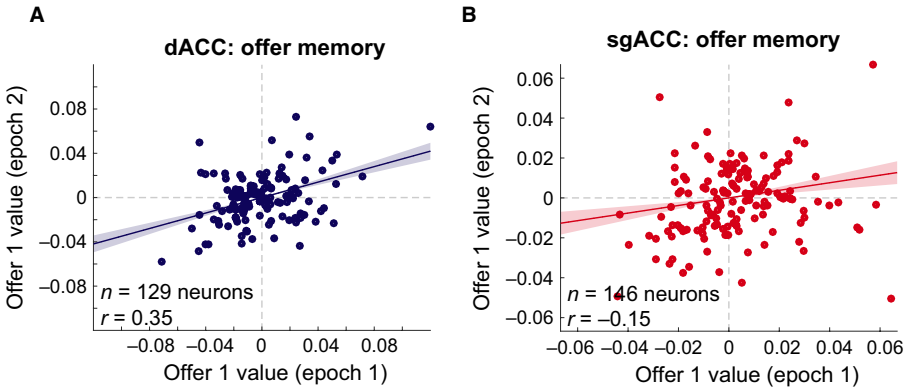

FIG. 5. Both regions encode the value of the first offer in similar formats across time. (A) Scatterplot of regression coefficients encoding the value of offer 1 when it is attended (epoch 1) and remembered (epoch 2) in dACC. Each dot represents the regression coefficients for a single neuron. The solid line indicates the mean Pearson's correlation across population regression coefficients, and the shaded region indicates the 99% credible interval of this measure. An analogous figure showing qualitatively similar results can be found in Azab & Hayden (2017). (B) Analogous scatterplot for sgACC.

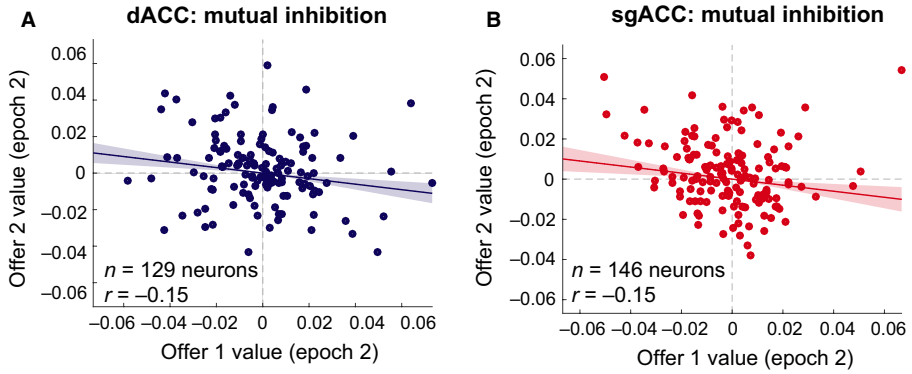

FIG. 6. Both regions encode the values of the two offers in opposing formats during comparison; a signature of value comparison (mutual inhibition). (A) Scatterplot of regression coefficients encoding the values of the two offers during comparison (epoch 2) in dACC. Each dot represents the regression coefficients for a single neuron. The solid line indicates the mean Pearson's correlation across population regression coefficients, and the shaded region indicates the 99% credible interval of this measure. An analogous figure showing qualitatively similar results can be found in Azab & Hayden (2017). (B) Analogous scatterplot for sgACC.

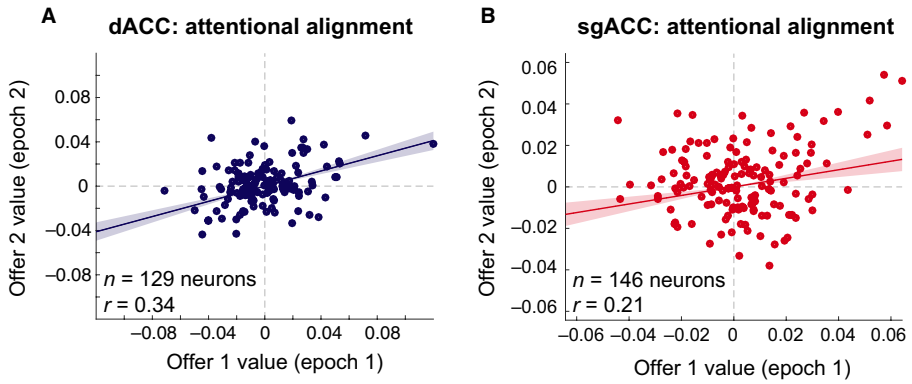

FIG. 7. Both regions encode the values of the two offers in similar formats while they are attended. (A) Scatterplot of regression coefficients encoding the values of the two offers in the respective epochs when they are attended (epoch 1 for offer 1, and epoch 2 for offer 2) in dACC. Each dot represents the regression coefficients for a single neuron. The solid line indicates the mean Pearson's correlation across population regression coefficients, and the shaded region indicates the 99% credible interval of this measure. An analogous figure showing qualitatively similar results can be found in Azab & Hayden (2017). (B) Analogous scatterplot for sgACC.

offers (dACC: $r = 0.303$, 99% credible interval = [0.200, 0.402]; sgACC: $r = 0.347$, 99% credible interval = [0.234, 0.459]). Qualitatively similar results were obtained using similar analyses with dACC data, and were reported in a previous article (Azab & Hayden, 2017).

Encoding of gamble outcomes and reward anticipation signals

We examined selectivity for gamble outcomes during the 700 ms reward epoch that began 100 ms after the reveal of the outcome and extended into the intertrial interval (see Fig. 1). Recall that trial-by-trial outcomes in this task were tokens, which were accumulated to obtain a juice rewards. Figure 8A and B show responses of two example neurones, one from each region, selective for outcome amount. 27.1% ($n = 35/129$) of neurones in dACC and 15.1% ($n = 22/146$) of neurones in sgACC encoded the outcome of a trial. Both of these proportions are significant (two-sided binomial test: $P = 1.11 \times 10^{-16}$ in dACC, $P = 3.97 \times 10^{-6}$ in sgACC). Figure 8C shows the peak of these fractions in the outcome epoch. These are the first demonstration of sgACC selectivity to gains or losses of secondary reinforcers.

Outcome-modulated neurones in dACC showed a slight positive bias in outcome encoding. Specifically, the majority of tuned neurones increased their firing rates with larger outcomes (68.6% positively tuned, $n = 24/35$; two-sided binomial test: $P = 0.0410$). However, this bias did not achieve significance in the overall population (Table 3). On the other hand, sgACC neurones showed a robust bias towards negative modulation in response to outcomes: both in the significantly modulated population (81.8% ($n = 18/22$) negatively tuned; two-sided binomial test: $P = 0.00434$), and in the overall population (Wilcoxon sign-rank test: $Z = -3.54$, $P = 0.000408$).

We also quantified neural responses to the anticipation of jackpots (large juice rewards) by comparing them to responses on standard trials (where no jackpot reward was obtained). Figure 9A and B show two example neurones—one from each region—with activity that varied with anticipation of a jackpot reward. Significant proportions of such neurones were found in both regions (37.2% in dACC, $n = 48/129$; two-sided binomial test: $P < 10^{-308}$; 12.3% in sgACC, $n = 18/146$; two-sided binomial test: $P = 0.0003890$). We saw no bias in positive or negative tuning in dACC: neither in the tuned population (Table 2), nor in the population overall (Table 3). However, there was a positive bias in sgACC modulation both in the significantly tuned population (83.35 ($n = 15/18$) positively modulated; two-sided binomial test: $P = 0.00754$) and in the overall population (Wilcoxon sign-rank test: $Z = 4.15$, $P = 3.38 \times 10^{-5}$), indicating

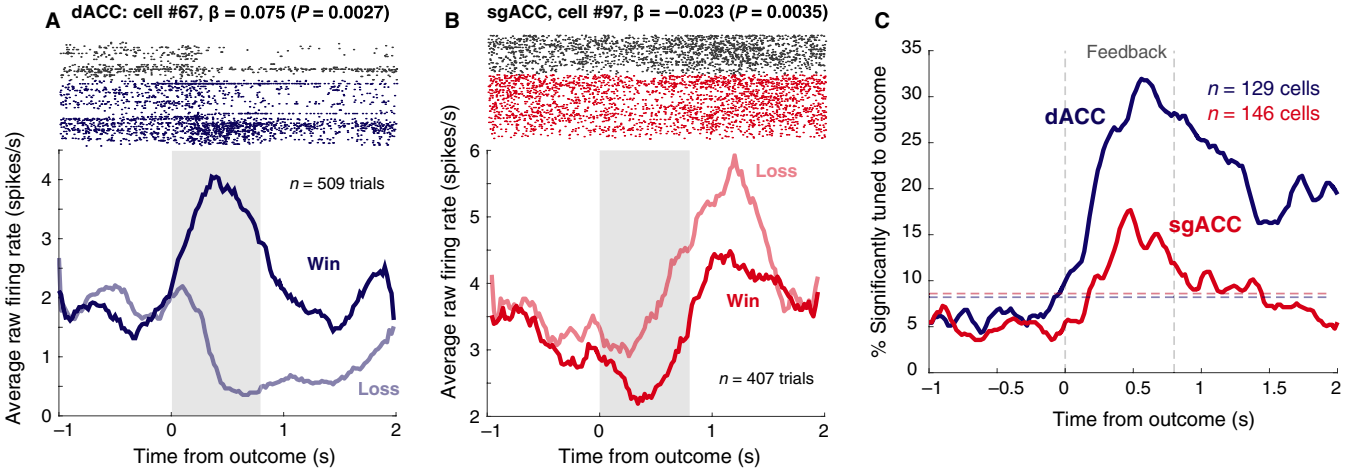

FIG. 8. Neural responses to outcomes in both regions. Grey shaded region indicates the time period during which feedback was displayed on the screen, as well as the subsequent delay prior to jackpot reward delivery/the subsequent trial. All standard errors of the mean were computed for the epoch of analysis (see main text and Methods). (A) dACC cell with increasing firing rate in response to wins. There was a slight bias towards this pattern in the population of dACC cells (see text and Table 2). Standard error of the mean for win trials = 0.513; standard error of the mean for loss trials = 0.194. (B) sgACC with increasing firing rate in response to losses. There was a bias towards this pattern in the population of sgACC neurons (see text and Tables 2 and 3). Standard error of the mean for win trials = 0.146; standard error of the mean for loss trials = 0.239. (C) Percentage of neurons in both regions tuned to the outcome of a trial throughout the course of a trial, using a 500 ms sliding window. The blue and red dashed lines indicate the percentage of neurons we would expect to see tuned by chance (as determined by a two-sided binomial test, according to the number of cells in each area) for dACC and sgACC, respectively. Recall that the significantly modulated populations showed a slight bias towards positive outcome encoding in dACC, and a significant bias towards negative outcome encoding in sgACC.

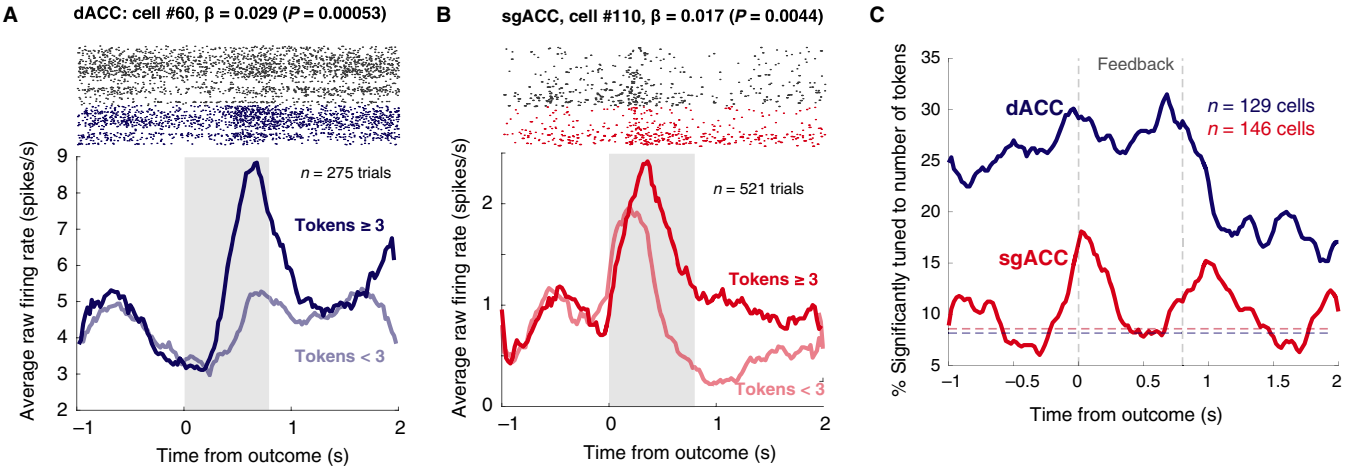

FIG. 9. Neural responses to the anticipation of a large liquid reward (jackpot). Grey shaded region indicates the time period during which feedback was displayed on the screen, as well as the subsequent delay prior to jackpot reward delivery/the subsequent trial. All standard errors of the mean were computed for the epoch of analysis (see main text and Methods). (A) dACC neuron that increased in firing rate before jackpot rewards. Time zero indicates the time the outcome is revealed. Standard error of the mean for jackpot trials = 1.17; standard error of the mean for non-jackpot trials = 0.349. (B) sgACC neuron that increased its firing rate before jackpot rewards. There was a bias towards this response profile in the sgACC population (see text and Tables 2 and 3). Standard error of the mean for jackpot trials = 0.335; standard error of the mean for non-jackpot trials = 0.0987. (C) Plot of the proportion of neurons selective for the outcome of the trial as a function of time relative to the outcome itself (time 0 indicates time outcome is revealed). Recall that the significantly modulated population in sgACC showed a significant bias towards positive responses in anticipation of a jackpot.

that sgACC neurones tend to fire more vigorously when anticipating primary rewards (as opposed to a new trial).

Neurones in both cingulate regions track progress through task towards primary reward

In our task, the number of tokens provided a measure of progress towards the jackpot reward. As shown above, task performance improved modestly with number of tokens. We hypothesized that this variable would affect neuronal responses in both cingulate areas. Figure 10A and B show two neurones (one in dACC, the other in sgACC) whose responses were modulated by the number of tokens acquired as of the start of the trial during the 700 ms reward epoch. 31.0% (n = 40/129) in dACC and 9.59% (n = 14/146) in sgACC significantly represented this variable in that epoch. Both of these fractions are significant (two-sided binomial test: $P < 10^{-308}$ in dACC and $P = 0.0157$ in sgACC). Figure 10C shows the change in this fraction throughout the trial. Note that the increase in significant

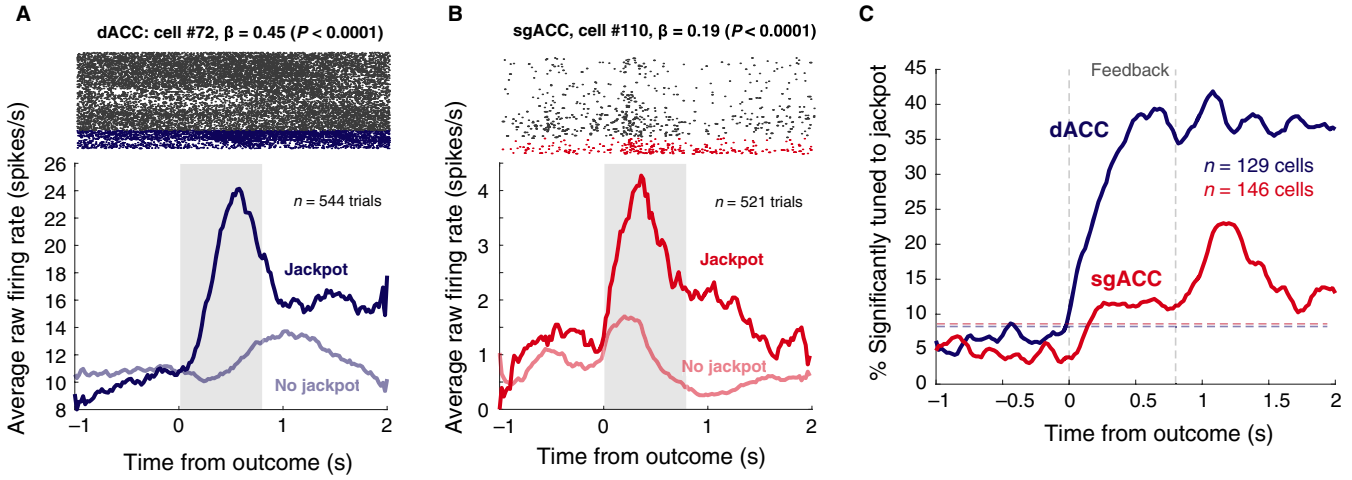

FIG. 10. Neural responses to the number of tokens accumulated at the beginning of the trial. Grey shaded region indicates the time period during which feedback was displayed on the screen, as well as the subsequent delay prior to jackpot reward delivery/the subsequent trial. All standard errors of the mean were computed for the epoch of analysis (see main text and Methods). (A) dACC cell that increased its firing rate as subjects accumulated more tokens. Standard error of the mean for high-token trials = 0.368; standard error of the mean for low-token trials = 0.292. (B) sgACC cell that increased its firing rate as subjects accumulated more tokens. Standard error of the mean for high-token trials = 0.190; standard error of the mean for low-token trials = 0.116. (C) Percentage of neurons in each area tuned to the number of tokens accumulated throughout the course of the trial. All percentages were computed using a 500 ms window (see Methods), with data-points centered around this window. The blue and red dashed lines indicate the percentage of neurons we would expect to see tuned by chance (as determined by a two-sided binomial test, according to the number of cells in each area) for dACC and sgACC, respectively.

modulation observed in the reward epoch cannot be attributed solely to a correlation between trial outcome and current number of tokens, as we regress neural activity against the number of tokens at the *start* of the trial, which is orthogonal to the outcome of that trial. There was a negative bias in modulation in the overall sgACC population (Wilcoxon sign-rank: $Z = -2.42$, $P = 0.0155$), although this bias did not extend to the significantly modulated population only (Table 2). dACC neurones exhibited no bias in modulation (Tables 2 and 3).

Neurones in both cingulate regions carry spatial signals

We previously showed coding for two task variables, spatial position of offer and chosen option, in both dACC and sgACC neurones (Strait *et al.*, 2016). The sgACC data used in that study ($n = 112$ neurones) were augmented with additional neurones collected in the same animals in the same task ($n = 34$ additional neurones; total of 146 neurones analysed in the present study). We still find these effects in the larger data set (note that for consistency with the other analyses in this article, we used a different analysis approach here than we did in that article, namely using a multiple regression analysis; see Methods). Specifically, sgACC encoded the position of the offer during the first offer epoch (8.90% ($n = 13/146$); two-sided binomial test: $P = 0.0368$), and the position of the chosen option during the post-choice epoch (11.6% ($n = 17/146$); two-sided binomial test: $P = 0.00107$). Results remained qualitatively similar in dACC with our new analyses. We see a significant proportion of neurones tuned to the side of the first offer in the first epoch (15.5% ($n = 20/129$); two-sided binomial test: $P = 6.88 \times 10^{-6}$), and to the side of the chosen offer in the post-choice epoch (19.4% ($n = 25/129$); two-sided binomial test: $P = 5.65 \times 10^{-9}$).

sgACC neurones encode the first offer value earlier than dACC neurones

Finally, we investigated latency differences between sgACC and dACC. Conventional latency analyses may be confounded due to the difference in signal-to-noise ratio between regions. In our data, signals are likely to achieve significance sooner in dACC, simply because they are stronger than in sgACC. To avoid this confound, we adopt a method fairly similar to that used by Siegel and colleagues (2015, see Methods). We see a significant difference in latency for the encoding of the first offer's value: significantly modulated sgACC neurones appear to encode this variable earlier than significantly modulated dACC neurones do (Wilcoxon rank-sum test: $Z = 2.98$, $P = 0.00292$; Fig. 11). Results were qualitatively similar when all neurones were used (Wilcoxon rank-sum test: $Z = 2.66$, $P = 0.00786$). No other reliable differences in latency were observed (Table 4).

Discussion

We characterized task-related responses of neurones in two cingulate regions, dACC and sgACC, in a token-gambling task. Neurones in both regions encode several task variables, including integrated offer values, primary as well as secondary outcomes, current progress in the task (in the form of the number of tokens acquired), and position of offered and chosen options. Both showed common coding schemes for the two offers; including correlates of working memory for the first offer's value, putative signatures of mutual inhibition (a correlate of value comparison) and an attentionally aligned (as opposed to labelled line) frame of evaluation (Azab & Hayden, 2017). These results demonstrate that key economic variables can be found both above and below the genu within the anterior cingulum. The set of variables encoded in these regions include many of those needed to implement economic decisions. These results, then, highlight the relatively close involvement of both regions in economic choice.

One similarity between the regions is particularly interesting to us: they both showed two signatures of value comparison we have reported in ventromedial pre-frontal area 14 (vmPFC, Strait *et al.*, 2014) and in ventral striatum (Strait *et al.*, 2015 VS). First, they both showed an anti-correlation between the regression weights for the values of the two offers at the time comparison likely occurred.

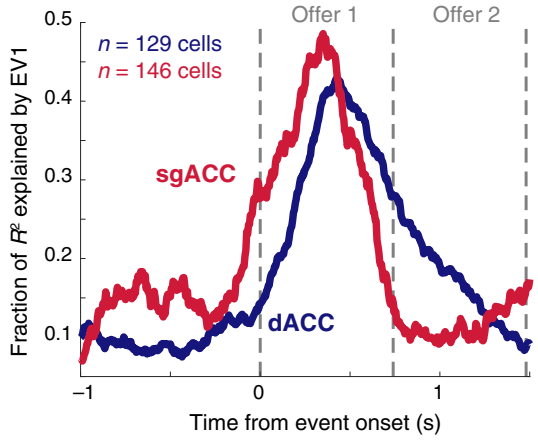

FIG. 11. Significantly modulated sgACC neurons encode the value of offer 1 earlier than dACC neurons. Plot shows the variance uniquely explained by the value of offer 1 throughout the course of the trial in each 500 ms window, sliding forward in 5 ms increments. Data-points are centered around this window.

TABLE 4. Latency of peak-encoding for each task variable in each brain region. Peak latency was estimated as the time-point where additional variance explained by this variable reached its peak. To test for significance, we perform a Wilcoxon sign-rank test on the peak latency of each significantly modulated neurone from both brain regions. Negative *Z*-statistics indicate that dACC neurones peaked earlier, while positive *Z*-statistics indicate that sgACC neurones peaked earlier.

Variable	Latency of peak average R^2		Wilcoxon rank-sum test *Z*-statistic (*P*-value)
	dACC	sgACC	
Offer 1 value (from offer 1 appearance)	473 ms	354 ms	**2.79 (*P* = 0.00530)**
Offer 2 value (from offer 2 appearance)	419 ms	340 ms	1.44 (*P* = 0.151)
Chosen side (from simultaneous appearance of options)	−209 ms	−219 ms	−0.118 (*P* = 0.906)
Number of tokens (from feedback)	356 ms	451 ms	−1.04 (*P* = 0.301)
Outcome (from feedback)	533 ms	510 ms	0.715 (*P* = 0.475)
Jackpot (from feedback)	545 ms	428 ms	1.95 (*P* = 0.052)

Values shown in bold indicate significant results.

This anti-correlation means that a value difference can be directly read out from a simple weighted average of neuronal responses, and is therefore an important decision variable for economic choice. The fact that such a signal is observed in four regions raises the possibility that value comparison occurs simultaneously across multiple brain regions (Hunt & Hayden, 2017). Second, both showed a tendency to encode the value of the attended option in a single format. Like the anti-correlation result, the same basic pattern was also observed in vmPFC and VS, and, in other work, in OFC (Blanchard *et al.*, 2015). Together, this work suggests that neurones throughout the reward system use attention, and not a labelled line system, as an organizational framework to determine value coding (Azab & Hayden, 2017). Note that this interpretation requires the assumption that the asynchronous presentation of options serves the purpose of controlling attention.

We observed two major differences between these regions. First, task-related signal-to-noise was consistently greater in dACC than in sgACC. One possible explanation for this finding is that sgACC has a broader repertoire than the functions measured by this task and that dACC uses its signals (perhaps among others) to generate a stronger representation of task variables. One reason for this would be that sgACC has a broader range of functions than dACC, including monitoring of other internal visceral variables we did not manipulate in our task (Bouret & Richmond, 2010). Second, we observed some differences in the average direction of value tuning: While sgACC encoding of both primary and secondary rewards was biased (towards increased responding to loss of secondary rewards and in anticipation of primary rewards), encoding in dACC neurones was fairly balanced. This organization is reminiscent of patterns of modulation in somatosensory cortex, where biases in modulation disappear in favour of more balanced responding as information flows up the cortical hierarchy (Romo & Salinas, 2001; Romo & Salinas, 2003). Another minor difference is that responses were slightly earlier in sgACC than dACC. This difference, while not dispositive, suggests that information about value (at least for offer 1, which we focused on), arrives earlier in sgACC than in dACC, and suggests a hierarchical organization. However, given that this is the only latency difference we observed, further study will be required to confirm this idea.

Our findings are consistent with the existing literature on sgACC. Monosov & Hikosaka (2012) find a bias towards encoding of negative outcomes in area 25. We show that this finding extends to secondary (token) reinforcers. They report no encoding of probability, and thus of integrated value; our tentative finding of integrated value encoding thus suggests that sgACC may play a more direct economic role than they proposed. One possible reason for the difference in findings is that our task requires a decision, which theirs did not; this requirement may have prompted sgACC to compute a decision variable directly usable in choice. In another study, Amemori & Graybiel (2012) recorded in pregenual cingulum, in a region that is rostral to our region, but that may have a small overlap (see Methods). They, too, found a subzone biased towards negative encodings. Our high fraction of subgenual neurones encoding upcoming large rewards (jackpots) provides single-neurone confirmation for the idea, proposed by Rudebeck and colleagues in their 2014 lesion study, that sgACC serves to sustain autonomic arousal in anticipation of a reward.

The phasic, task-relevant signals in sgACC, and its direct role in reward processing and anticipation, suggest that the role of subgenual neurones extends beyond the control of basic arousal functions such as sleep (Rolls *et al.*, 2003). On the other hand, we believe that our results align well with those obtained in a study by Bouret & Richmond (2010). They reported strong encoding of internal variables, such as satiety, in a region they call vmPFC, but that likely includes some of our recording sites (and extends ventrally and a bit laterally). They contrasted these findings with those obtained in OFC, which had more externally driven responses. Given that our task focuses on external variables, the weaker encoding of those variables in sgACC echoes their result. In conjunction with their finding, our results raise the possibility that sgACC serves as an initial site at which internal and external variables may be bound into value variables that can influence choice.

The bias we detected towards increased responding to negative outcomes also coheres with the findings relating activity in sgACC to negative affect and depression. Overactivity in this region correlates with depressive symptoms (Mayberg *et al.*, 2000; Drevets, 2002) and with transient sadness in healthy subjects (Mayberg *et al.*, 1999). Chronic stimulation of sgACC can also alleviate the symptoms of depression (Mayberg *et al.*, 2005). Negative mood inducing

stimuli tend to activate sgACC (Mayberg *et al.*, 1997, 1999; George *et al.*, 2006), and structural abnormalities in sgACC correlate with mood disorders (Drevets *et al.*, 1997; Botteron *et al.*, 2002; Coryell *et al.*, 2005).

Our work provides some support for the idea that dACC participates in choice, but suggests it may not be the sole site at which choice occurs (Hunt & Hayden, 2017). Our results, which show encoding of pre-decisional variables, argue against the idea that dACC plays a largely post-decisional role (Blanchard & Hayden, 2014; Azab & Hayden, 2017). Our work also provides some support for the idea that the role of dACC in persistence is signalling the value of the upcoming offer (Shidara & Richmond, 2002; Picton *et al.*, 2007; Chudasama *et al.*, 2013; Hillman & Bilkey, 2013; Blanchard *et al.*, 2015).

Our findings of functional overlap in dACC and sgACC provide some support for the idea that the anterior cingulum may have a single discrete function above and beyond the distinct roles of its subregions. We speculate that this function includes the integration of diverse inputs—cognitive, limbic and otherwise—to influence ongoing decisions. This hypothesis also leaves room for the differences observed between dACC and sgACC in neuroimaging and lesion studies (reviewed in Bush *et al.*, 2000 & Paus, 2001), as well as differences in anatomical connectivity (Devinsky *et al.*, 1995; Heilbronner & Haber, 2014), as regions are proposed to serve distinct functions that, combined, serve an overarching process (Wilson *et al.*, 2010). The question, then, is what this overarching process may be, if it exists, for the cingulate cortex. As such, a future goal of our research programme is to extend our investigation to other cingulate regions, especially the posterior cingulate cortex (PCC). Neural responses in the dorsal posterior cingulate gyrus (which we have called CGp) are associated with several economic variables, including offer and outcome variables, as well as learning and control variables (McCoy *et al.*, 2003; McCoy & Platt, 2005; Pearson *et al.*, 2009; Hayden *et al.*, 2010; Heilbronner *et al.*, 2011; Heilbronner & Platt, 2013). These results hint at a broader transcingulate function.

Another open question is how specific functions associated with the cingulate may or may not differ from those associated with the broader pre-frontal cortex. We have recorded outside the cingulum in reward-sensitive cortex in ventromedial pre-frontal cortex (vmPFC) and in orbitofrontal cortex (OFC) in structurally similar tasks (Strait *et al.*, 2014; Blanchard *et al.*, 2015; Wang & Hayden, 2017). Results from those studies indicate that many of the economic variables observed in the cingulum are also found outside of it. These findings in turn raise the possibility that economic choice involves the coordinated activation of multiple brain regions, including both cingulate and non-cingulate.

Supporting Information

Additional supporting information can be found in the online version of this article:

Data S1. Accounting for saccade latencies.

Acknowledgements

This research was supported by an NIH R01 (DA037229) and an NSF CAREER award to BYH. We thank Caleb Strait for assistance designing the task, Tommy Blanchard, Frank Mollica and Alex Thomé for useful discussions, and Meghan Castagno, Giuliana Loconte and Marc Mancarella for assistance in data collection.

Conflict of interest statement

The authors declare no conflict of interest.

Data accessibility

All data is available on the data section of the Hayden Lab website (www.haydenlab.com/datacode.html).

Author contributions

B.Y.H led the design of the task. H.A. assisted with data collection. H.A. performed all data analyses. H.A. and B.Y.H. wrote and edited the manuscript.

Abbreviations

CGp, posterior cingulate gyrus; dACC, dorsal anterior cingulate cortex; ITI, intertrial interval; OFC, orbitofrontal cortex; PCC, posterior cingulate cortex; pgACC, pregenual anterior cingulate cortex; sgACC, subgenual anterior cingulate cortex; vmPFC, ventromedial pre-frontal cortex; VS, ventral striatum.

References

Amemori, K.I. & Graybiel, A.M. (2012) Localized microstimulation of primate pregenual cingulate cortex induces negative decision-making. *Nat. Neurosci.*, **15**, 776–785.

Amiez, C., Joseph, J.P. & Procyk, E. (2005) Reward encoding in the monkey anterior cingulate cortex. *Cereb. Cortex*, **16**, 1040–1055.

Azab, H. & Hayden, B.Y. (2017) Correlates of decisional dynamics in the dorsal anterior cingulate cortex. *PLoS Biol.*, **15**, e2003091.

Blanchard, T.C. & Hayden, B.Y. (2014) Neurons in dorsal anterior cingulate cortex signal postdecisional variables in a foraging task. *J. Neurosci.*, **34**, 646–655.

Blanchard, T.C. & Hayden, B.Y. (2015) Monkeys are more patient in a foraging task than in a standard interremporal choice task. *PLoS One*, **10**, e0117057.

Blanchard, T.C. Piantadosi, S.T. & Hayden, B.Y. (2018) Robust mixture modeling reveals category free selectivity in reward region neuronal ensembles. *J. Neurophysiol. In press.*

Blanchard, T.C., Wilke, A. & Hayden, B.Y. (2014) Hot hand bias in rhesus monkeys. *J. Exp. Psychol. – Anim. L.*, **40**, 280–286.

Blanchard, T.C., Strait, C.E. & Hayden, B.Y. (2015) Ramping ensemble activity in dorsal anterior cingulate neurons during persistent commitment to a decision. *J. Neurophysiol.*, **114**, 2439–2449.

Boorman, E.D., Rushworth, M.F. & Behrens, T.E. (2013) Ventromedial prefrontal and anterior cingulate cortex adopt choice and default reference frames during sequential multi-alternative choice. *J. Neurosci.*, **33**, 2242–2253.

Botteron, K.N., Raichle, M.E., Drevets, W.C., Heath, A.C. & Todd, R.D. (2002) Volumetric reduction in left subgenual prefrontal cortex in early onset depression. *Biol. Psychiat.*, **51**, 342–344.

Bouret, S. & Richmond, B.J. (2010) Ventromedial and orbital neurons differentially encode internally and externally driven motivation values in monkeys. *J. Neurosci.*, **30**, 8591–8601.

Brainard, D.H. (1997) The psychophysics toolbox. *Spat. Vis.*, **10**, 433–436.

Bush, G., Luu, P. & Posner, M.I. (2000) Cognitive and emotional influences in anterior cingulate cortex. *Trends Cogn. Sci.*, **4**, 215–222.

Bush, G., Vogt, B.A., Holmes, J., Dale, A.M., Greve, D., Jenike, M.A. & Rosen, B.R. (2002) Dorsal anterior cingulate cortex: a role in reward-based decision making. *Proc. Natl. Acad. Sci. USA*, **99**, 523–528.

Cai, X. & Padoa-Schioppa, C. (2012) Neuronal encoding of subjective value in dorsal and ventral anterior cingulate cortex. *J. Neurosci.*, **32**, 3791–3808.

Chudasama, Y., Daniels, T.E., Gorrin, D.P., Rhodes, S.E., Rudebeck, P.H. & Murray, E.A. (2013) The role of the anterior cingulate cortex in choices based on reward value and reward contingency. *Cereb. Cortex*, **23**, 2884–2898.

Cornelissen, F.W., Peters, E.M. & Palmer, J. (2002) The Eyelink Toolbox: eye tracking with MATLAB and the psychophysics toolbox. *Behav. Res. Methods*, **34**, 613–617.

Coryell, W., Nopoulos, P., Drevets, W., Wilson, T. & Andreasen, N.C. (2005) Subgenual prefrontal cortex volumes in major depressive disorder and schizophrenia: diagnostic specificity and prognostic implications. *Am. J. Psychiat.*, **162**, 1706–1712.

Cotter, D., Mackay, D., Landau, S., Kerwin, R. & Everall, I. (2001) Reduced glial cell density and neuronal size in the anterior cingulate cortex in major depressive disorder. *Arch. Gen. Psychiat.*, **58**, 545–553.

Derbyshire, S.W.G., Vogt, B.A. & Jones, A.K.P. (1998) Pain and Stroop interference tasks activate separate processing modules in anterior cingulate cortex. *Exp. Brain Res.*, **118**, 52–60.

Devinsky, O., Morrell, M.J. & Vogt, B.A. (1995) Contributions of anterior cingulate cortex to behaviour. *Brain*, **118**, 279–306.

Donahue, C.H. & Lee, D. (2015) Dynamic routing of task-relevant signals for decision making in dorsolateral prefrontal cortex. *Nat. Neurosci.*, **18**, 295–301.

Drevets, W. (2002) Functional anatomical correlates of antidepressant drug treatment assessed using PET measures of regional glucose metabolism. *Eur. Neuropsychopharmacol.*, **12**, 527–544.

Drevets, W.C., Price, J.L., Simpson, J.R. Jr, Todd, R.D., Reich, T., Vannier, M. & Raichle, M.E. (1997) Subgenual prefrontal cortex abnormalities in mood disorders. *Nature*, **386**, 824.

Ebitz, R.B. & Hayden, B.Y. (2016) Dorsal anterior cingulate: a Rorschach test for cognitive neuroscience. *Nat. Neurosci.*, **19**, 1278–1279.

Forman, S.D., Dougherty, G.G., Casey, B.J., Siegle, G.J., Braver, T.S., Barch, D.M., ... Lorensen, E. (2004) Opiate addicts lack error-dependent activation of rostral anterior cingulate. *Biol. Psychiat.*, **55**, 531–537.

Fuster, J.M. (2001) The prefrontal cortex—an update: time is of the essence. *Neuron*, **30**, 319–333.

George, M.S., Ketter, T.A., Parekh, P.I., Horwitz, B., Herscovitch, P. & Post, R.M. (2006) Brain activity during transient sadness and happiness in healthy women. *Am. J. Psychiat.*, **152**, 341–351.

Goldstein, R.Z., Tomasi, D., Rajaram, S., Cottone, L.A., Zhang, L., Maloney, T., Telang, F., Alia-Klein, N. *et al.* (2007) Role of the anterior cingulate and medial orbitofrontal cortex in processing drug cues in cocaine addiction. *J. Neurosci.*, **144**, 1153–1159.

Grueschow, M., Polania, R., Hare, T.A. & Ruff, C.C. (2015) Automatic versus choice-dependent value representations in the human brain. *Neuron*, **85**, 874–885.

Haber, S.N. & Behrens, T.E. (2014) The neural network underlying incentive-based learning: implications for interpreting circuit disruptions in psychiatric disorders. *Neuron*, **83**, 1019–1039.

Hare, T.A., Schultz, W., Camerer, C.F., O'Doherty, J.P. & Rangel, A. (2011) Transformation of stimulus value signals into motor commands during simple choice. *Proc. Natl. Acad. Sci.*, **108**, 18120–18125.

Hayden, B.Y., Heilbronner, S.R., Nair, A.C. & Platt, M.L. (2008) Cognitive influences on risk-seeking by rhesus macaques. *Judgm Decis Mak.*, **3**, 389.

Hayden, B.Y. & Platt, M.L. (2007) Temporal discounting predicts risk sensitivity in rhesus macaques. *Curr. Biol.*, **17**, 49–53.

Hayden, B.Y., Pearson, J.M. & Platt, M.L. (2011) Neuronal basis of sequential foraging decisions in a patchy environment. *Nat. Neurosci.*, **14**, 933.

Hayden, B., Smith, D.V. & Platt, M. (2010) Cognitive control signals in posterior cingulate cortex. *Front Hum. Neurosci.*, **4**, 223.

Heilbronner, S.R. & Haber, S.N. (2014) Frontal cortical and subcortical projections provide a basis for segmenting the cingulum bundle: implications for neuroimaging and psychiatric disorders. *J. Neurosci.*, **34**, 10041–10054.

Heilbronner, S.R. & Hayden, B.Y. (2016) Dorsal anterior cingulate cortex: a bottom-up view. *Annu. Rev. Neurosci.*, **39**, 149–170.

Heilbronner, S., Hayden, B.Y. & Platt, M. (2011) Decision salience signals in posterior cingulate cortex. *Fronti. Neurosci.*, **5**, 55.

Heilbronner, S.R. & Platt, M.L. (2013) Causal evidence of performance monitoring by neurons in posterior cingulate cortex during learning. *Neuron*, **80**, 1384–1391.

Hillman, K.L. & Bilkey, D.K. (2010) Neurons in the rat anterior cingulate cortex dynamically encode cost–benefit in a spatial decision-making task. *J. Neurosci.*, **30**, 7705–7713.

Hillman, K.L. & Bilkey, D.K. (2013) Persisting through subjective effort: A key role for the anterior cingulate cortex? *Behav. Brain Sci.*, **36**, 691–692.

Hunt, L.T. & Hayden, B.Y. (2017) A distributed, hierarchical and recurrent framework for reward-based choice. *Nat. Rev. Neurosci.*, **18**, 172–182.

Ito, S., Stuphorn, V., Brown, J.W. & Schall, J.D. (2003) Performance monitoring by the anterior cingulate cortex during saccade countermanding. *Science*, **302**, 120–122.

Johansen-Berg, H., Gutman, D.A., Behrens, T.E.J., Matthews, P.M., Rushworth, M.F.S., Katz, E., Lozano, A.M., Mayberg, H.S. (2008) Anatomical connectivity of the subgenual cingulate region targeted with deep brain stimulation for treatment-resistant depression. *Cereb. Cortex*, **18**, 1374–1383.

Klein-Flügge, M.C., Kennerley, S.W., Friston, K. & Bestmann, S. (2016) Neural signatures of value comparison in human cingulate cortex during decisions requiring an effort-reward tradeoff. *J. Neurosci.*, **36**, 10002–10015.

Kriegeskorte, N., Mur, M. & Bandettini, P.A. (2008) Representational similarity analysis-connecting the branches of systems neuroscience. *Front. Syst. Neurosci.*, **2**, 4.

Lak, A., Stauffer, W.R. & Schultz, W. (2014) Dopamine prediction error responses integrate subjective value from different reward dimensions. *Proc. Natl. Acad. Sci. USA*, **111**, 2343–2348.

Mante, V., Sussillo, D., Shenoy, K.V. & Newsome, W.T. (2013) Context-dependent computation by recurrent dynamics in prefrontal cortex. *Nature*, **503**, 78–84.

Maxwell, S.E. & Delaney, H.D. (1993) Bivariate median splits and spurious statistical significance. *Psychol. Bull.*, **113**, 181–190.

Mayberg, H.S., Brannan, S.K., Mahurin, R.K., Jerabek, P.A., Brickman, J.S., Tekell, J.L., Silva, J.A., McGinnis, S. *et al.* (1997) Cingulate function in depression: a potential predictor of treatment response. *NeuroReport*, **8**, 1057.

Mayberg, H.S., Liotti, M., Brannan, S.K., McGinnis, S., Mahurin, R.K., Jerabek, P.A., ... Fox, P. T. (1999) Reciprocal limbic-cortical function and negative mood: converging PET findings in depression and normal sadness. *Am. J. Psychiat.*, **156**, 675–682.

Mayberg, H.S., Brannan, S.K., Tekell, J.L., Silva, J.A., Mahurin, R.K., McGinnis, S. & Jerabek, P.A. (2000) Regional metabolic effects of fluoxetine in major depression: serial changes and relationship to clinical response. *Biol. Psychiat.*, **48**, 830–843.

Mayberg, H.S., Lozano, A.M., Voon, V., McNeely, H.E., Seminowicz, D., Hamani, C., Schwalb, J.M., Kennedy, S.H. (2005) Deep brain stimulation for treatment-resistant depression. *Neuron*, **45**, 651–660.

McCoy, A.N. & Platt, M.L. (2005) Risk-sensitive neurons in macaque posterior cingulate cortex. *Nat. Neurosci.*, **8**, 1220–1227.

McCoy, A.N., Crowley, J.C., Haghighian, G., Dean, H.L. & Platt, M.L. (2003) Saccade reward signals in posterior cingulate cortex. *Neuron*, **40**, 1031–1040.

Miller, E.K. & Cohen, J.D. (2001) An integrative theory of prefrontal cortex function. *Annu. Rev. Neurosci.*, **24**, 167–202.

Monosov, I.E. & Hikosaka, O. (2012) Regionally distinct processing of rewards and punishments by the primate ventromedial prefrontal cortex. *J. Neurosci.*, **32**, 10318–10330.

Niki, H. & Watanabe, M. (1979) Prefrontal and cingulate unit activity during timing behavior in the monkey. *Brain Res.*, **171**, 213–224.

O'Doherty, J.P. (2004) Reward representations and reward-related learning in the human brain: insights from neuroimaging. *Curr. Opn. Neurobiol.*, **14**, 769–776.

O'reilly, R.C., Noelle, D.C., Braver, T.S. & Cohen, J.D. (2002) Prefrontal cortex and dynamic categorization tasks: representational organization and neuromodulatory control. *Cereb. Cortex*, **12**, 246–257.

Paus, T. (2001) Primate anterior cingulate cortex: where motor control, drive and cognition interface. *Nat. Rev. Neurosci.*, **2**, 417–424.

Paxinos, G., Huang, X.F. & Toga, A.W. (2000). *The Rhesus Monkey Brain in Stereotaxic Coordinates*. Academic Press, San Diego, USA.

Pearson, J.M., Hayden, B.Y., Raghavachari, S. & Platt, M.L. (2009) Neurons in posterior cingulate cortex signal exploratory decisions in a dynamic multioption choice task. *Curr. Biol.*, **19**, 1532–1537.

Picton, T.W., Stuss, D.T., Alexander, M.P., Shallice, T., Binns, M.A. & Gillingham, S. (2007) Effects of focal frontal lesions on response inhibition. *Cereb. Cortex*, **17**, 826–838.

Rolls, E.T., Inoue, K. & Browning, A. (2003) Activity of primate subgenual cingulate cortex neurons is related to sleep. *J. Neurophysiol.*, **90**, 134–142.

Romo, R. & Salinas, E. (2001) Touch and go: decision-making mechanisms in somatosensation. *Annual Rev. Neurosci*, **24**, 107–137.

Romo, R. & Salinas, E. (2003) Cognitive neuroscience: flutter discrimination: neural codes, perception, memory and decision making. *Nat. Rev. Neurosci.*, **4**, 203.

Rudebeck, P.H., Putnam, P.T., Daniels, T.E., Yang, T., Mitz, A.R., Rhodes, S.E. & Murray, E.A. (2014) A role for primate subgenual cingulate cortex in sustaining autonomic arousal. *Proc. Natl. Acad. Sci. USA*, **111**, 5391–5396.

Rushworth, M.F.S., Hadland, K.A., Paus, T. & Sipila, P.K. (2002) Role of the human medial frontal cortex in task switching: a combined fMRI and TMS study. *J. Neurophysiol.*, **87**, 2577–2592.

Rushworth, M.F., Noonan, M.P., Boorman, E.D., Walton, M.E. & Behrens, T.E. (2011) Frontal cortex and reward-guided learning and decision-making. *Neuron*, **70**, 1054–1069.
Rustichini, A. & Padoa-Schioppa, C. (2015) A neuro-computational model of economic decisions. *J. Neurophysiol.*, **114**, 1382–1398.
Schultz, W. (2000) Multiple reward signals in the brain. *Nature Rev Neurosci.*, **1**, 199.
Seo, H. & Lee, D. (2007) Temporal filtering of reward signals in the dorsal anterior cingulate cortex during a mixed-strategy game. *J. Neurosci.*, **27**, 8366–8377.
Shenhav, A., Botvinick, M.M. & Cohen, J.D. (2013) The expected value of control: an integrative theory of anterior cingulate cortex function. *Neuron*, **79**, 217–240.
Shidara, M. & Richmond, B.J. (2002) Anterior cingulate: single neuronal signals related to degree of reward expectancy. *Science*, **296**, 1709–1711.
Siegel, M., Buschman, T.J. & Miller, E.K. (2015) Cortical information flow during flexible sensorimotor decisions. *Science*, **348**, 1352–1355.
Stokes, M.G., Kusunoki, M., Sigala, N., Nili, H., Gaffan, D. & Duncan, J. (2013) Dynamic coding for cognitive control in prefrontal cortex. *Neuron*, **78**, 364–375.
Strait, C.E., Blanchard, T.C. & Hayden, B.Y. (2014) Reward value comparison via mutual inhibition in ventromedial prefrontal cortex. *Neuron*, **82**, 1357–1366.
Strait, C.E., Sleezer, B.J. & Hayden, B.Y. (2015) Signatures of value comparison in ventral striatum neurons. *PLoS Biol.*, **13**, e1002173.
Strait, C.E., Sleezer, B.J., Blanchard, T.C., Azab, H., Castagno, M.D. & Hayden, B.Y. (2016) Neuronal selectivity for spatial positions of offers and choices in five reward regions. *J. Neurophysiol.*, **115**, 1098–1111.
Vogt, B.A., Finch, D.M. & Olson, C.R. (1992) Functional heterogeneity in cingulate cortex: the anterior executive and posterior evaluative regions. *Cereb. Cortex*, **2**, 435–443.
Walton, M.E., Groves, J., Jennings, K.A., Croxson, P.L., Sharp, T., Rushworth, M.F. & Bannerman, D.M. (2009) Comparing the role of the anterior cingulate cortex and 6-hydroxydopamine nucleus accumbens lesions on operant effort-based decision making. *Eur. J. Neurosci.*, **29**, 1678–1691.
Walton, M.E., Kennerley, S.W., Bannerman, D.M., Phillips, P.E.M. & Rushworth, M.F. (2006) Weighing up the benefits of work: behavioral and neural analyses of effort-related decision making. *Neural Networks*, **19**, 1302–1314.
Wang, M. Z. & Hayden, B. Y. (2017) Reactivation of associative structure specific outcome responses during prospective evaluation in reward-based choices. *Nat. Commun.*, **8**, ncomms15821.
Wilson, C.R., Gaffan, D., Browning, P.G. & Baxter, M.G. (2010) Functional localization within the prefrontal cortex: missing the forest for the trees? *Trends Neurosci.*, **33**, 533–540.
Wunderlich, K., Rangel, A. & O'Doherty, J.P. (2009) Neural computations underlying actionbased decision making in the human brain. *Proc. Natl. Acad. Sci.*, **106**, 17199–17204.
Yamada, H., Tymula, A., Louie, K. & Glimcher, P.W. (2013) Thirst-dependent risk preferences in monkeys identify a primitive form of wealth. *Proc. Natl. Acad. Sci. USA*, **110**, 15788–15793.

Graphical Abstract

The contents of this page will be used as part of the graphical abstract of html only. It will not be published as part of main article.

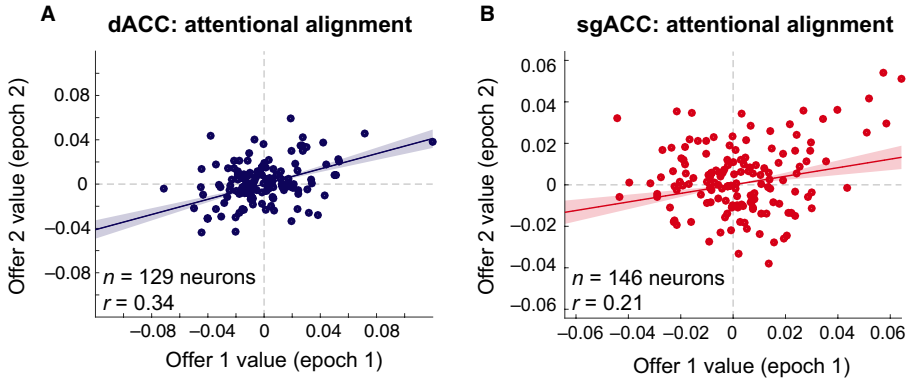

The role of the anterior cingulate in cognition has been hotly debated. This study shows that neurons in both the dorsal and subgenual regions encode key economic variables, and exhibit correlates of value comparison. Nonetheless, responses across regions do exhibit subtle differences; the subgenual shows more biased responding to reward variables than the dorsal, suggestive of a distributed network for value-based decision-making, and perhaps a hierarchy of information flow.